Statistical assessment of total heat losses from externally finned tubes using various spatially weighted mean Biot numbers

Antonio Campo
College of Engineering, Idaho State University, Pocatello, ID, USA

Luis R. Pericchi
Departamento de Matemáticas, Universidad Simón Bolívar, Caracas, Venezuela

The present work considers a theoretical analysis of the heat transfer augmentation of in-tube flows due to the addition of an array of fins at the outer surface of the tube. The fins having annular shape and constant thickness are uniformly spaced in the heat-exchange region. The aim of the article is to examine the thermal response of various spatial-weighted mean values of the axially varying external convective coefficient within the framework of statistical analysis. It was found that the arithmetic spatial mean and the geometrical spatial mean of the external convective coefficient provide accurate estimates of the upper and lower bounds, respectively, for the exact heat transfer rates. This finding, in conjunction with the use of an approximate lumped-parameter model for the energy conservation equation, permits a simplistic algebraic evaluation of the thermal performance of this kind of externally finned tube with different geometrical and thermal arrangements. A complete set of results is presented in graphical form and can be used for optimization of cooling processes.

Keywords: externally finned tubes; mean Biot numbers; lumped-parameter model

Introduction

Substantial heat transfer augmentation in forced-convection pipe flow may be achieved by fitting a regularly spaced array of annular fins (externally), as compared with the baseline situation of a bare pipe without fins. Correspondingly, the degree of heat transfer augmentation is sensitive to the combined influence of the convective coefficient for the unfinned segment, h_1, and the equivalent convective coefficient for the finned segment, h_2, as well as the associated fin thickness, x_2, and the interfin spacing, x_1, respectively. In particular, the use of air-cooled condensing units in industry has spurred considerable interest in this subject. Therefore, the mean bulk temperature distribution along with the total heat removal relevant to the cooling of an internal fluid flow moving in a finned tube depend strongly on these four quantities. Unquestionably, the primary design consideration for engineering problems is the rate at which heat can be extracted by attaching a fin array.

From a fundamental point of view, this internal forced-convection problem may be regarded as a thermal entrance problem being subject to a boundary condition of the third kind, where the external convective coefficient h_e varies periodically (and abruptly) in the streamwise direction of the pipe. The above-cited problem, under the assumption that a hydrodynamically developed situation prevails, has led many researchers to use analytical methods (Vick and Wells 1986; Vick et al. 1987; Santos et al. 1988) and numerical techniques (Sparrow and Charmchi 1980) to incorporate the external finning effects into the heat transfer analysis. In general, these elaborate procedures are quite limited in their applicability, and for computational purposes are very time consuming.

Additionally, it was also realized by Sparrow and Charmchi (1980) that the finite-difference computational task was quite demanding because the abrupt changes in Bi (see Figure 1) required a very fine distribution of grid points. In light of this, to complement and provide perspective to the numerical results, additional numerical solutions based on a constant Biot number (invariant with the axial coordinate) were carried out by these authors. Indeed, the adoption of a constant Biot number corresponds to an arithmetic spatial mean accounting for Bi_1 and Bi_2 in the unfinned (low value) and finned (high value) surfaces of the pipe, as well as the corresponding fin thickness and the interfin spacing. In principle, this alternative route served to simplify the wall boundary condition drastically, because the periodic variation of the convective coefficient $h_e(x)$ at the pipe surface was replaced by a constant convective coefficient. Hence, within the context of convective heat transfer theory, the original problem has been successfully reduced to a classical Graetz problem having a standard boundary condition of the third kind. In this regard, it should be mentioned that an analytical solution of this transformed

Address reprint requests to Dr. Campo at College of Engineering, Idaho State University, Pocatello, ID 83209, USA.

Received 22 September 1991; accepted 25 February 1992

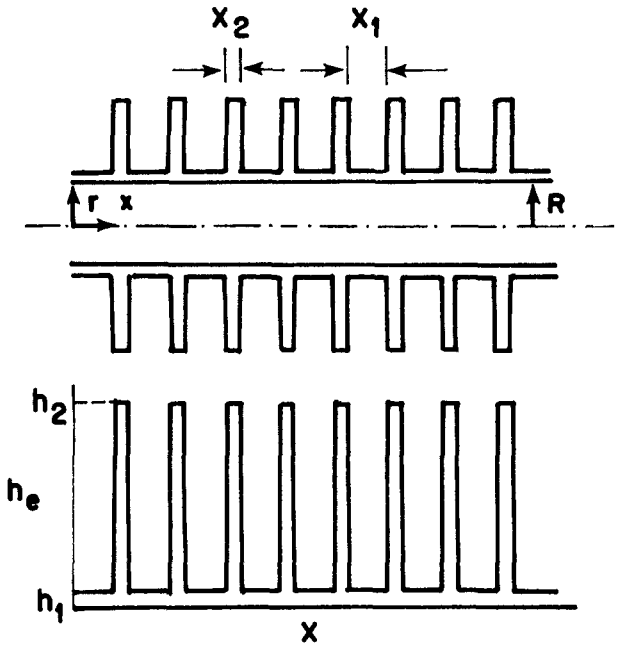

Figure 1 Schematic view of the finned tube

problem, via eigenquantities, has been presented by Ozisik and Sadeghipour (1982).

Conversely, Sparrow and Charmchi (1980) also suggested that as an alternate procedure to the arithmetic spatial mean of the Biot number, a force-fit calculation approach might have been taken. Accordingly, a succession of constant-Biot-number solutions would have been run until an equivalent Biot value was found that yielded a satisfactory fit with the results of the variable-Biot-number case, accounting for different fin thickness and interfin spacings. However, this force-fit approach was considered extremely costly with regard to computer storage and time, and it would have practical merit only if the force-fit Biot numbers could be adequately correlated with Bi_1, Bi_2, X_1, and X_2. Evidently, as Sparrow and Charmchi (1980) pointed out, the existence of such a correlation equation can only be explored by solving an extremely large number of cases accounting for all possible combinations, and for this reason it was abandoned and not employed.

Turning the attention to the alternative approach involving the arithmetic spatial mean of the Bi number proposed originally by Sparrow and Charmchi (1980), its most significant detraction is that the computed heat transfer rates in the thermal entry region of finned pipes are always overestimated in comparison to the corresponding exact rates based on the actual periodically changing Bi number. In fact, these overestimations (upper bounds) tend to be more pronounced in the vicinity of the pipe inlet ($x = 0$) for practical situations in which the differences between Bi_1 and Bi_2 increase. As a result, this evidence, in conjunction with the uncertainty in the heat transfer rates, strongly suggest that the mean Biot number is the thermophysical property most in need of investigation.

Little is known concerning the formal statistical aspects of the spatial-mean Biot number as applicable to externally finned pipes, since these effects have not been studied extensively in the literature. Therefore, additional fundamental investigations of the potential spatial-mean values are needed for purposes of thermal design of heat-exchange devices. The realization of their full potential requires practical engineering models that are capable of estimating both the maximum and minimum heat transport processes accurately.

In view of the foregoing limitations involving the arithmetic spatial mean of the Biot number, namely Bi_a, the primary aim of this article is to deduce and test a variety of weighted spatial means of Bi within the framework of statistical analysis that may provide reliable upper and lower bounds for the laminar forced convection in externally finned pipes. The intent here is not to simulate realistically the thermal system itself, but to

Notation

Bi	Biot number, $h_e R/k$
Bi_1	Biot number for unfinned surface, $h_1 R/k$
Bi_2	Biot number for finned surface, $h_2 R/k$
Bi_a	Arithmetic spatial mean of Bi
Bi_g	Geometric spatial mean of Bi
Bi_h	Harmonic spatial mean of Bi
c_p	Specific heat of internal fluid
D	Pipe diameter
$E(g)$	Mean of g, Equation 6
$g(X)$	Function, Equation 5
h_e	Local value of the external convective coefficient
$\bar{h}_e$	Spatial-mean value of h_e
h_1	External convective coefficient for unfinned surface
h_2	External convective coefficient for finned surface
h_i	Internal convective coefficient
k	Thermal conductivity of internal fluid
L	Pipe length
$\bar{L}$	Dimensionless value of L, $L/R\mathrm{Pe}$
$\dot{m}$	Mass flow rate of internal fluid
$M_r(g)$	Generalized spatial mean of g, Equation 8
$\underline{Nu}_i$	Local value of the internal Nusselt number, $h_i D/k$
$\overline{Nu}_i$	Average value of Nu_i
Nu_{eq}	Local value of the equivalent Nusselt number, Equation 19b
$\overline{Nu}_{eq}$	Average value of Nu_{eq}
$p(X)$	Function, Equation 4
Pe	Peclet number of internal fluid, $\bar{u}D/\alpha$
Q_T	Total heat transfer, Equation 24
r	Index, Equation 8
R	Pipe radius
T_b	Mean bulk temperature of internal fluid
T_0	Inlet fluid temperature at $x = 0$
T_∞	Stagnant temperature of external fluid
$\bar{u}$	Mean velocity of internal fluid
U	Local value of the overall heat transfer coefficient, Equation 16
$V(g)$	Variance of g, Equation 5
x	Axial coordinate
x_1	Interfin segment
x_2	Fin segment
X	Dimensionless axial coordinate, $x/R\mathrm{Pe}$
X_1	Dimensionless value of x_1
X_2	Dimensionless value of x_2

Greek letters

α	Thermal diffusivity of internal fluid
θ_b	Dimensionless value of T_b, $(T_b - T_0)/(T_\infty - T_0)$
Λ	Heat transfer efficiency, Equation 25
ρ	Density of internal fluid

assess the relative importance of statistically determined bounds. The details of the statistical methodology are described in the next section. In the later section devoted to the presentation of results, comparisons have been made with the exact calculation procedure in order to establish a range of geometrical and thermal parameters for which the proposed statistically determined bounds are accurate.

Throughout the present study, it is also shown that a relatively simple mathematical model can be adequately used to predict correct physical trends in external, annular, finned pipes and is capable of a broad range of applications. As indicated by Vick and Wells (1986), Vick et al. (1987), Santos et al. (1988), and Sparrow and Charmchi (1980), the consensus is that good accuracy has been observed and at the same time considerable savings in storage and computational costs have been obtained in comparison with the complete differential formulation and calculation procedure accounting for variable $\mathrm{Bi}(x)$ numbers. The approximate and simplistic lumped-parameter model provides realistic upper and lower bounds for the total heat transfer rates irrespective of the values of the controlling geometrical and thermal parameters.

Statistical analysis

The lower portion of Figure 1 illustrates the model adopted for the axially varying heat removal at the outer surface of a circular tube having ring-shaped fins. In this figure, the external convective coefficient h_e is simply modeled as a periodic variation of low values, h_1 (associated with the unfinned segment x_1), and high values, h_2 (associated with the finned segment x_2), respectively. These thermal variables may be recast in dimensionless form as two different Biot numbers, namely,

$$\mathrm{Bi}_1 = \frac{h_1 R}{k} \qquad \mathrm{Bi}_2 = \frac{h_2 R}{k} \tag{1}$$

which have to be related to the successive dimensionless portions of the tube:

$$X_1 = \frac{x_1}{R\,\mathrm{Pe}} \qquad X_2 = \frac{x_2}{R\,\mathrm{Pe}} \tag{2}$$

respectively.

With a view of simplifying the mathematical formulation and finding a means of circumventing the lengthy calculations accounting for the abrupt and periodic variation of the Biot number $\mathrm{Bi}(X)$ as already mentioned, constant-Biot-number solutions were sought by Sparrow and Charmchi (1980). Accordingly, these authors proposed an arithmetic spatial mean of the Biot number, which is designated in this article by Bi_a. It is given by the expression

$$\mathrm{Bi}_a = \frac{(X_1\,\mathrm{Bi}_1 + X_2\,\mathrm{Bi}_2)}{(X_1 + X_2)} \tag{3}$$

Based on their computed results, this approximation was found to consistently overestimate the total heat transfer in this kind of finned pipe because, from the statistical standpoint, it was systematically biased upwards in all the graphical comparisons made. The largest deviations consistently occur near the inlet of the heat-exchange section of the tube ($x = 0$) and, as expected, lesser deviations appear at larger downstream distances ($x \gg 0$).

In view of the fact that the arithmetic spatial mean, Bi_a, utilized by Sparrow and Charmchi (1980) does not provide satisfactory heat transfer results with the rigorous and formal analysis via a periodic variation, $\mathrm{Bi}(X)$, we proceeded here to define a generalized spatial weighted mean of Bi_1 and Bi_2 in order to select dependable spatial means that may provide bounding curves for the "exact" results. Correspondingly, these generalized spatial means will automatically incorporate expressions relating them with the participating geometrical and thermal parameters, namely, Bi_1, X_1, Bi_2, and X_2, respectively.

First, assuming the existence of a uniform distribution in a certain interval between $X = 0$ and $X = X_1 + X_2$, we may construct the function

$$p(X) = \begin{cases} \dfrac{1}{X_1 + X_2} & \text{for } 0 \leqslant X \leqslant X_1 + X_2 \\ 0 & \text{otherwise} \end{cases} \tag{4}$$

As a result of this, we may also define another function $g(X)$, such that

$$g(X) = \begin{cases} \mathrm{Bi}_1 & \text{for } 0 \leqslant X \leqslant X_1 \\ \mathrm{Bi}_2 & \text{for } X_1 \leqslant X \leqslant X_1 + X_2 \\ 0 & \text{otherwise} \end{cases} \tag{5}$$

Consequently, the mean of $g(X)$ is the arithmetic spatial mean expressed by the relation

$$\begin{aligned} E[g] &= \int_{-\infty}^{\infty} g(X)p(X)\,dX \\ &= \frac{1}{X_1 + X_2}\left[\int_0^{X_1} g(X)\,dX + \int_{X_1}^{X_1+X_2} g(X)\,dX\right] \\ &= \frac{X_1\,\mathrm{Bi}_1 + X_2\,\mathrm{Bi}_2}{X_1 + X_2} = \mathrm{Bi}_a \end{aligned} \tag{6}$$

In addition, the associated variance $V(g)$ of the function $g(X)$—in other words, Bi_a—may be expressed as follows:

$$\begin{aligned} V(g) &= E[g^2] - E^2[g] \\ &= \frac{1}{X_1 + X_2}(X_1\,\mathrm{Bi}_1^2 + X_2\,\mathrm{Bi}_2^2) - \mathrm{Bi}_a^2 \\ &= \frac{X_1 X_2}{(X_1 + X_2)}(\mathrm{Bi}_1 - \mathrm{Bi}_2)^2 \end{aligned} \tag{7}$$

Thus, a simple inspection of the preceding equation reveals that the variance, $V(g)$, increases whenever $(\mathrm{Bi}_1 - \mathrm{Bi}_2)^2$ increases, ultimately reaching its maximum value for the particular case where $X_1 \gg X_2$ (unfinned segment larger than the finned segment). Moreover, it may also be observed that for a large difference between Bi_1 and Bi_2 and whenever $X_1 \gg X_2$, the magnitude of the variance $V(g)$ seems to be an appreciable quantity. Consequently, under these extreme but realistic circumstances, it is readily concluded that based on the sole behavior of the variance, the arithmetic spatial mean, Bi_a, by itself gives a poor approximation of a periodic functional variation of $\mathrm{Bi}(X)$ in the entire interval: $0 < X < \infty$. Notice that the heat liberation takes place in this interval.

In view of the foregoing limitation, let us proceed to define here a generalized spatial mean, namely, $M_r(g)$ of $g(X)$, as follows:

$$\begin{aligned} M_r(g) &= \left[\int_{-\infty}^{+\infty} g^r(X)p(X)\,dX\right]^{1/r} \\ &= \left\{\frac{1}{X_1 + X_2}\left[\int_0^{X_1} g^r(X)\,dX + \int_{X_1}^{X_1+X_2} g^r(X)\,dX\right]\right\}^{1/r} \\ &= \left(\frac{X_1\,\mathrm{Bi}_1^r + X_2\,\mathrm{Bi}_2^r}{X_1 + X_2}\right)^{1/r} \end{aligned} \tag{8}$$

Correspondingly, the next step in the systematic statistical development is to choose a numerical value of the index or exponent r ($-\infty \leqslant r \leqslant \infty$) that enables the generation of better approximations for any imposed periodic function of $\mathrm{Bi}(X)$. For instance, with the foregoing as a background, two different means may be readily constructed. These are

(1) the arithmetic spatial mean for $r = +1$:

$$\mathrm{Bi}_a = M_1(g)$$

$$\mathrm{Bi}_a = \frac{X_1\,\mathrm{Bi}_1 + X_2\,\mathrm{Bi}_2}{X_1 + X_2} \tag{9}$$

(2) the harmonic spatial mean for $r = -1$:

$$\mathrm{Bi}_h = M_{-1}(g)$$

$$\mathrm{Bi}_h = \left[\frac{1}{X_1 + X_2}\left(\frac{X_1}{\mathrm{Bi}_1} + \frac{X_2}{\mathrm{Bi}_2}\right)\right]^{-1} \tag{10}$$

Furthermore, in addition to these two spatial-means values, the geometric spatial mean, Bi_g, described by the relation

$$\mathrm{Bi}_g = (\mathrm{Bi}_1^{X_1}\,\mathrm{Bi}_2^{X_2})^{1/(X_1+X_2)} \tag{11}$$

may also be obtained from the generalized spatial mean defined in Equation 8 as the index r tends to zero. At this stage, it should be appropriate to add that the required step-by-step procedure for the determination of Equation 11, as well as the rigorous mathematical proof, can be found in Hardy, Littlewood, and Polya (1967).

Conversely, from a broad perspective of the theory on generalized spatial means, several important relations for the Biot number may be delineated as follows:

$$\mathrm{Bi}_g = \lim_{r\to 0} M_r(g) \tag{12a}$$

$$\mathrm{Bi}_1 = \lim_{r\to +\infty} M_r(g) \tag{12b}$$

$$\mathrm{Bi}_2 = \lim_{r\to -\infty} M_r(g) \tag{12c}$$

Moreover, if $r_2 < r_1$, then we may also write that

$$M_{r_2}(g) < M_{r_1}(g) \tag{13}$$

Therefore, by virtue of these concepts, it follows that the three spatial-mean values cited in the preceding paragraph are quantitatively related by the two inequalities

$$\mathrm{Bi}_a > \mathrm{Bi}_g > \mathrm{Bi}_h \tag{14a}$$

and

$$\mathrm{Bi}_2 < M_r(g) < \mathrm{Bi}_1 \tag{14b}$$

covering in this way all finite values of the index r.

Physical significance

As already stated in the introduction, the present research was undertaken to determine not a single bound, but a definite band comprising upper and lower bounds for the estimation of the thermal performance of externally finned tube flows.

Considering the fluid/fin space as a control volume, the arithmetic-spatial-mean Bi_a gives the "overall conductivity" if the heat transport in the fluid and the solid medium is arranged in "parallel." In contrast, if the heat transport in the fluid and solid medium is entirely in "series," the harmonic-spatial-mean Bi_h characterizes this configuration. From physical grounds, Bi_a and Bi_h definitely constitute the upper and lower bounds, respectively, of the overall conductivity. In consequence, the parallel arrangement should offer the least thermal resistance to heat transport, whereas the series arrangement is indicative of the greatest thermal resistance.

By virtue of Equation 14a, it is clear that the geometric-spatial-mean Bi_g is always intermediate in value between the two extremes Bi_a and Bi_h, suggesting that it may well be another restrictive candidate for the bounding analysis of this study. However, to test this suggestion, the formulas for Bi_a, Bi_g, and Bi_h have to be applied concurrently to the data taken from Sparrow and Charmchi (1980) and Vick and Wells (1986). These authors provided the exact solution to the problem.

Lumped-parameter methodology

The physical situation under study in this article is shown schematically in Figure 1. In this investigation, a circular pipe fitted with a regularly spaced array of transverse external, annular fins rejects heat to the surrounding fluid maintained at a uniform temperature, T_∞. Under the assumption that a fully developed laminar velocity and a uniform temperature T_0 prevail at the inlet of the heat-exchange section $x = 0$, the heat loss to the surrounding fluid takes place through a sequence of unfinned and finned portions of the pipe. Hence, as clearly depicted in Figure 1b, this thermal interaction between the internal and external fluids basically corresponds to abrupt changes of low and high values of external convective coefficients h_1 and h_2, applied at the respective interfin and fin segments, x_1 and x_2.

Variation of the bulk temperature

Motivated by the success of the lumped-energy formulation in the study of laminar forced-convection pipe flows (Campo and Lacoa 1987; Lacoa and Campo 1990), this simplified formulation will be also adopted here to test the worth of various candidate spatial-weighted means developed in the preceding section. For first-order analysis of engineering problems, however, the lumped-system model is often preferred, because it provides the correct physical trends and requires less effort and expense. Accordingly, neglecting axial conduction effects and performing a lumped-energy balance on a typical control volume inside the pipe yields the ordinary differential equation of first order:

$$\frac{dT_b}{dx} = -\frac{4U}{\rho c_p \bar{u} D}(T_b - T_\infty) \tag{15}$$

Here, T_b is the mean bulk temperature characterizing the internal fluid flow in the appropriate control volume and U is the overall heat transfer coefficient linking the local heat-exchange process at any x from the internal fluid to the external fluid. The boundary condition imposed on Equation 15 is $T_b = T_0$ at $x = 0$.

By virtue of the definition of U (Incropera and DeWitt 1990), this thermal quantity may be rewritten and expressed compactly in terms of the local internal Nusselt number and the external local value of the Biot number as follows:

$$U = \frac{\dfrac{k}{D}}{\dfrac{1}{\mathrm{Nu}_i} + \dfrac{1}{2\mathrm{Bi}}} \tag{16}$$

where k is the thermal conductivity of the internal fluid. Correspondingly, to be consistent with the lumped-system formulation, it is necessary that the relations for both Nu_i and

Bi must conform with the condition that an isothermal wall temperature, T_w, prevails in the control volume.

Firstly, focusing attention on the external fluid, the abrupt variation of Bi with X (see Figure 1, lower portion) corresponds to an axially periodic distribution of the external convective coefficient h_e. Secondly, directing the attention to the internal fluid stream, the local Nusselt number, Nu_i, shows a monotonic decreasing change with X. Consequently, from a mathematical perspective, both Bi and Nu_i render a position-dependent character to U, which may be expressed in functional form as $U = U(x)$.

In light of this, the dimensionless lumped-energy equation (Equation 15), along with its boundary condition, may be recast as follows:

$$\frac{d\theta_b}{dX} = 2Nu_{eq}(1 - \theta_b), \qquad \theta_b(0) = 0 \tag{17}$$

where the participating dimensionless variables are

$$\theta_b = \frac{T_b - T_0}{T_\infty - T_0} \quad \text{and} \quad X = \frac{x}{R\,Pe} \tag{18}$$

Furthermore, in Equation 17,

$$Nu_{eq} = \frac{UD}{k} \tag{19a}$$

designates an equivalent Nusselt number that governs the interconnection between the internal-convection and the external-convection phenomena through the fin array and the surrounding fluid, respectively. Hence, this number may be computed by the relation

$$\frac{1}{Nu_{eq}} = \frac{1}{Nu_i} + \frac{1}{2Bi} \tag{19b}$$

Thus, from a statistical point of view, Equation 19b identifies a harmonic mean between Nu_i and 2Bi, which in turn is responsible for the characterization of the heat transfer process, respectively. As a consequence of this rearrangement, since Nu_{eq} replaces U, the former becomes a strong and complicated function of the dimensionless axial coordinate, X, as well.

Uniform external convective coefficient

The objective now is to focus on a further simplification of the mathematical formulation of the forced-convection problem under study here. Within this context, consideration will be given to the definition of the overall heat transfer coefficient, U, written in Equation 16. Here, the axial variation of Bi will be replaced by effective spatial Biot numbers given by Equations 9 through 11, which are in fact axially invariant. In addition, following this idea, Equation 16 may be simplified even more by supplanting the distribution of the isothermal-wall local Nusselt number, $Nu_i(X)$, by the corresponding distribution of the average Nusselt number, $\overline{Nu}_i(L)$. To accomplish this goal, the correlation equation developed by Hausen (1943) may be utilized directly—that is,

$$\overline{Nu}_i = 3.657 + \frac{0.134/\bar{L}}{1 + 0.064/\bar{L}^{2/3}} \tag{20}$$

where $\bar{L} = L/R\,Pe$ denotes the dimensionless axial station. Most recently, Gnielinski (1989) has proposed a single comprehensive equation, covering a wider range of Prandtl number fluids, that is an extension of Equation 20.

Accordingly, this alternate route, based on a position-independent value of U, provides also a position-independent value of the equivalent-average Nusselt number, $\overline{Nu}_{eq}$:

$$\overline{Nu}_{eq} = \frac{1}{\dfrac{1}{\overline{Nu}_i} + \dfrac{1}{2Bi}} \tag{21}$$

where the lumped-energy equation (Equation 17) may be rewritten as follows:

$$\frac{d\theta_b}{dX} = 2\overline{Nu}_{eq}(1 - \theta_b), \qquad \theta_b(0) = 0 \tag{22}$$

As may be observed, this equation constitutes a separable ordinary differential equation of first order because $\overline{Nu}_{eq}$ is now a constant, and not a function of X, as was the case in Equation 19b. Therefore, after performing the direct integration, the closed-form solution is

$$\theta_b(\bar{L}) = 1 - \exp(-2\overline{Nu}_{eq}\bar{L}) \tag{23}$$

Undoubtedly, the numerical evaluation of Equation 23 is straightforward and may be carried out by hand without utilizing an integration scheme, such as Runge–Kutta on a computer. Therefore, by choosing various axial stations, $\bar{L}$, in the downstream portion of the finned pipe, a mean bulk temperature distribution $\theta_b(\bar{L})$ may be plotted right away by simply combining algebraically an appropriate spatial-mean Biot number with Equations 20, 21, and 23.

Total heat removal

From a practical standpoint, the thermal quantity of paramount importance in this problem is the total heat removal, Q_T, from the fluid flowing through the finned tube to the surrounding medium between any two stations, $x = 0$ and $x = L$. This quantity may be easily calculated, via a global energy balance, and written as

$$Q_T = \dot{m}c_p[T_0 - T_b(L)] \tag{24}$$

where T_0 is the temperature of the internal fluid at the inlet of the heat exchange region $x = 0$. Alternatively, upon introduction of a heat transfer efficiency or dimensionless heat transfer Λ, Equation 24 becomes

$$\Lambda = \frac{Q_T}{\dot{m}c_p(T_0 - T_\infty)} = \theta_b(\bar{L}) \tag{25}$$

where $\theta_b(\bar{L})$ designates the dimensionless bulk temperature at any streamwise station, $X = \bar{L}$. Thus, knowledge of θ_b at any pre-selected downstream station, $\bar{L}$, is synonymous with the total heat transferred, Q_T, up to the station (see Equation 24), without the necessity of calculating and plotting an additional thermal quantity, usually the distribution of the finned-tube Nusselt number Nu_x.

Discussion of results

To illustrate the application and to limit the volume of numerical results that may be needed, we consider the cases described in Table 1. Under the assumption of equally spaced fins, these cases seek to cover a wide range of conditions for different combinations of the interfin spacing X_2 and the fin Biot number Bi_1. For comparison purposes in Cases 2 to 4, the "exact" results, as well as the approximate results based on the spatial-arithmetic-mean Bi_a, have been taken from the comprehensive publication by Sparrow and Charmchi (1980). These authors utilized a finite-volume procedure and a high

Table 1 Combination of geometrical and thermal parameters considered

Case	X_1	Bi_1	X_2	Bi_2	Bi_a	Bi_g	Bi_h
2a	3×10^{-4}	1	10^{-4}	20	5.75	2.11	1.31
2b	3×10^{-4}	1	10^{-4}	50	13.25	2.66	1.32
2c	3×10^{-4}	1	10^{-4}	100	25.75	3.16	1.33
3a	7×10^{-4}	1	10^{-4}	20	3.38	1.45	1.13
3b	7×10^{-4}	1	10^{-4}	50	7.13	1.63	1.14
3c	7×10^{-4}	1	10^{-4}	100	13.38	1.78	1.14
4a	10^{-4}	1	10^{-4}	20	10.50	4.47	1.90
4b	10^{-4}	1	10^{-4}	50	25.50	7.07	1.96
4c	10^{-4}	1	10^{-4}	100	50.50	10.00	1.98
5a	3×10^{-3}	1	10^{-3}	20	5.75	2.11	1.31
5b	3×10^{-3}	1	10^{-3}	50	13.25	2.66	1.32
5c	3×10^{-3}	1	10^{-3}	100	25.75	3.16	1.33

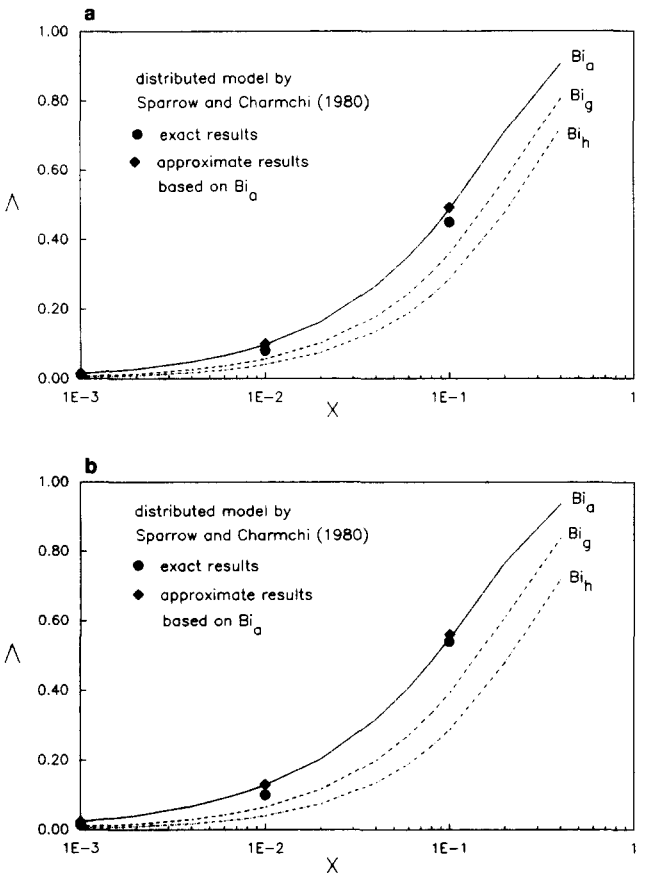

Figure 2 Bounding curves for the total heat liberation related to case 2

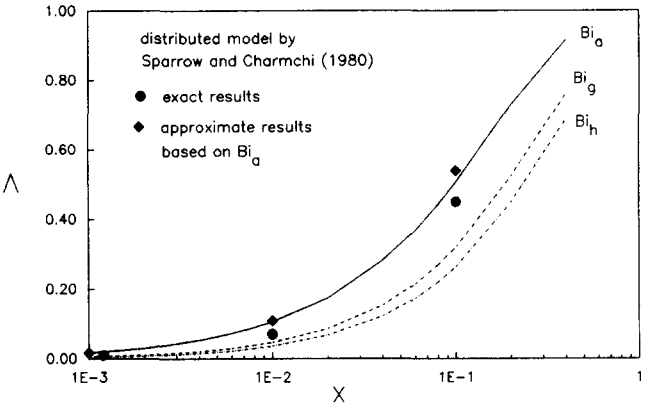

Figure 3 Bounding curves for the total heat liberation related to case 3

population of nodes for the solution of the distributed 2-D energy equation subject to a stepwise periodic variation of the external convective coefficient. Similarly, for Case 5, the analytical results of Vick and Wells (1986) will be used for comparison purposes. In this investigation, a variable eigenfunction technique for the distributed 2-D energy equation was employed, resulting in a system of coupled first-order ordinary differential equations. This system was eventually solved numerically on a computer. In this regard, it should be stressed that comparison results for the arithmetic-spatial-mean Biot number were not presented by Vick and Wells (1986).

From a general view of Figures 2, 3, and 4, it is seen that the heat transfer distributions follow a consistent and expected pattern. In each family of curves, the upper curve is associated with the arithmetic spatial mean, the middle curve represents the geometric spatial mean, and the lower curve is concerned with the harmonic spatial mean. In essence, this sweeping behavior is in accordance with the outcome of the systematic statistical analysis expressed by Inequality 14a, whereby the heat transfer rate is maximum for Bi_a, intermediate for Bi_g, and minimum for Bi_h. In theory, we should anticipate that the "exact" heat transfer rates based on the spacewise variation of $Bi = Bi(X)$ will lie somewhere in between the above-cited extreme conditions. In practice, it has been already demonstrated by the outcome of Sparrow and Charmchi (1980) that the arithmetic-spatial-mean Bi_a constitutes an upper bound for the thermal performance of finned tubes. However, aside from the fact that Bi_a constitutes an upper bound, an important question that needs to be answered is whether the geometric or the harmonic spatial mean (Bi_g or Bi_h) yields a realistic and dependable lower bound. Undoubtedly, this crucial lower bound is an indispensable thermal quantity for the safe thermal analysis and design of finned tubes, because it provides the minimum possible heat removal. Consequently, to address this issue thoroughly, a detailed comparative study involving the "exact" results computed by Sparrow and Charmchi (1980) and Vick et al. (1986) and the three approximate predictive statistical models needs to be made. In what follows, the heat transfer results will be presented graphically with the heat transfer efficiency Λ along the ordinate and the dimensionless axial position X along the abscissa. The set of computed results will be parameterized by X_1, X_2, Bi_1, and Bi_2, as indicated in Table 1. In the characterization of the curves, the designations

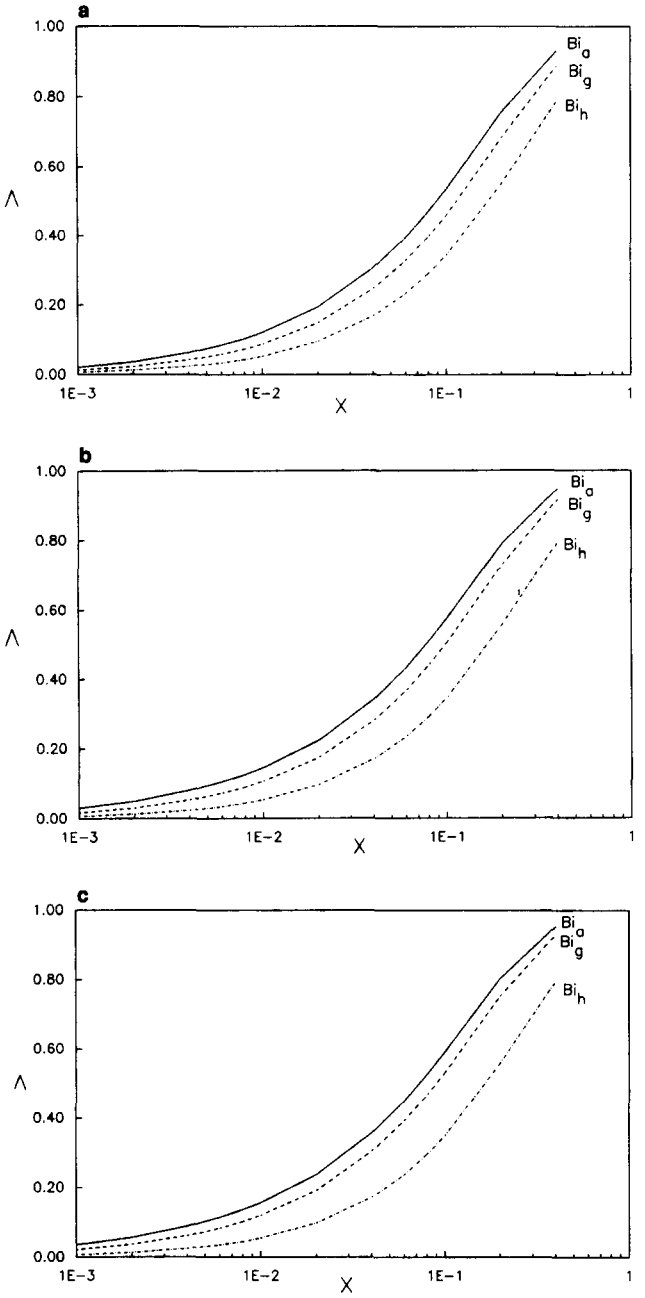

Figure 4 Bounding curves for the total heat liberation related to case 4

Bi_a, Bi_g, and Bi_h, respectively, refer to the estimated results via the lumped formulation. Additionally, the filled circles are used to convey the "exact" results, whereas the filled diamonds represent the upper-bound results, relying on the arithmetic spatial mean. For simplicity, these data points are taken from the publication of Sparrow and Charmchi (1980) at three different axial stations only. Initial attention will be given to Case 2 and its associated Figures 2a and 2b, illustrating geometrical situations wherein the interfin spacing X_1 is three times the fin thickness X_2.

An overview of Figure 2a clearly indicates that the "exact" results are perfectly bounded by the set of approximate limiting results given by Bi_a and Bi_g, respectively. For all values of X, it is seen that the former correspond to an upper bound, whereas the latter correspond to a lower bound. In addition, the bounding curve for Bi_a does not appear to be sensitive to the solution procedure utilized, that is, either distributed or lumped formulations. In Figure 2b, the effects of Bi_2 can be further explored. For this situation, $Bi_2 = 50$, and the results corresponding to a higher fin heat transfer follow exactly the same pattern as those of Figure 2a. Therefore, the response of heat transfer rates set forth in connection with Figure 2a may now be regarded as a firmer conclusion.

Case 3 depicts the variation of Λ with X for an interfin spacing of $X_1 = 7 \times 10^{-4}$. The only reported values for $X_1 = 7 \times 10^{-4}$ are those for $Bi_2 = 50$. These values are plotted in Figure 3 along with the present bounding results. The trend of the family of three curves in Figure 2 persists. As seen in Figure 3, the Bi_a results obtained by both methods are consistently above the "exact" values. With regard to these, at any X the individual deviations from the Bi_a curve are less sensitive than the corresponding deviations from the Bi_g curve. The results of Case 3 can be put into quantitative perspective by noting that, during various levels of cooling, the predictive band tends to widen as Bi_2 increases from 20 to 100. This is not shown so as to conserve journal space.

Figure 4 conveys results of a further exploration of the influence of the interfin spacing in the external fin bundle. As far as the confidence limits are concerned, the interfin spacing plays a very significant role in the forced-convection problem. Under the special conditions of fin thickness equal to the interfin spacing ($X_1 = X_2 = 10^{-4}$), the typical variations of Λ *versus* X are shown in Figure 4. No known theoretical work has been reported about the local heat transfer distributions on the finned side. From a general view of Figure 4 it is noted that, under these circumstances, the uncertainty region shrinks to a very narrow band. This band seems to be unaltered by the drastic changes of Bi_2 ranging from 20 to 100. Due to the close proximity of the Λ-curves for Bi_a and Bi_g, it may be firmly concluded that they indeed serve to estimate rather accurately the "exact" results (via an algebraic equation) as long as $X_1 = X_2$.

For completeness purposes, it is also interesting to compare the present set of approximate results with those made by Vick and Wells (1986). For further analysis of the statistically determined bounds, calculations have been made for Case 5, wherein $X_1 = 3 \times 10^{-3}$ and $X_2 = 10^{-3}$. Note that these numerical values have an order of magnitude less than those related to Case 2. To initiate the discussion, Figure 5a shows the consistent correlation between the "exact" results computed by Vick and Wells (1986) for $Bi_2 = 20$ and the approximate estimates provided by the use of the bounds Bi_a and Bi_g in the lumped-based formulation. With a further increase in Bi_2 to 50, the heat transfer behavior in Figure 5b does not change significantly from that observed before in Figure 5a. At this point, the only observation that is worth mentioning is that the "exact" results lean toward those associated with the lower bound, i.e., Bi_g, in contrast with the behavior seen in Figure 2b.

Ultimately, a comparison between Cases 2 and 5 in Table 1 seems to be logical from the standpoint of statistical analysis per se. Both cases are identical, except for the fact that the geometrical parameters X_1 and X_2 differ by a factor of 10. A detailed inspection of the last three columns clearly reveals that the numerical values of the spatial-mean Biot numbers are similar for each corresponding combination of geometrical and thermal parameters. Therefore, it is possible to establish an equivalent Biot-number ratio—for instance, Bi_2/Bi_1—that governs this convection problem related to externally, annular finned tubes. This finding is a useful concept for practical designs and can be easily corroborated by comparing independent runs. Specifically, Figures 2 and 5 indicate an interesting phenomenon: the Λ-values for the two bounding

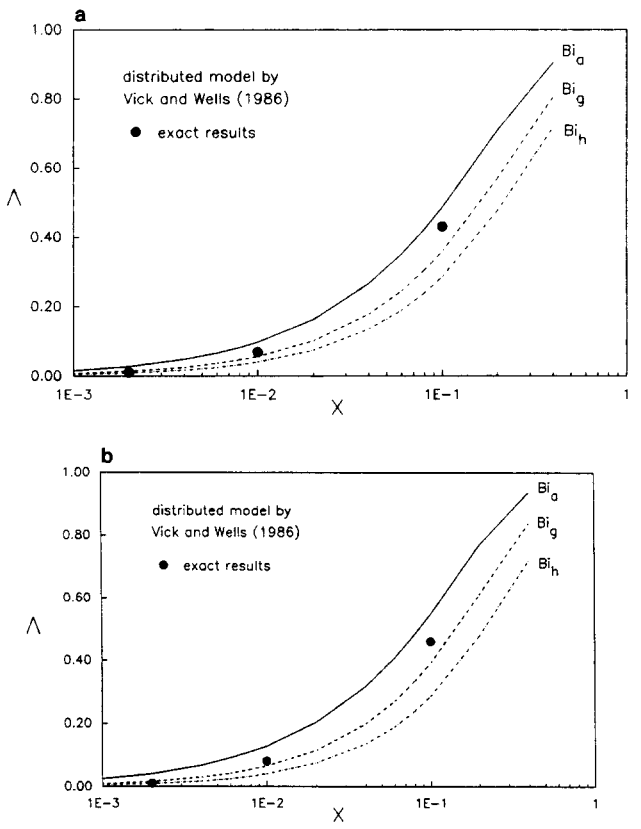

Figure 5 Bounding curves for the total heat liberation related to case 5

curves based on X_2/X_1 = constant are identical as long as the values for Bi_1 and Bi_2 remain unchanged. Practical use of this equivalence would be that present design criteria can be extended to account for other geometrical conditions relying on a single set of predictive curves without carrying out additional calculations.

Concluding remarks

This article presents a simple mathematical model to establish the limits of the total heat transfer that takes place in a circumferentially finned tube, thereby obviating the need for tedious and complicated finite-difference calculations using a computer code. The proposed methodology yields algebraically determined results that are physically realistic for all considered cases involving various geometric and/or thermal parameters. The main bulk temperature distributions are given in the form of simple functions.

The primary contribution of this study is to provide a measure of the deviation of the estimated Λ-distributions from the true "exact" Λ-distributions. The theoretical results clearly show that the geometric-spatial-mean Bi_g, not the harmonic-spatial-mean Bi_h, is the deciding parameter in the prediction of minimum heat transfer rates. This claim has been convincingly validated.

Due to the complex nature of the problem, the bounding results can be used in place of the "exact" results for most problems of practical interest. The outcome of this comparative study may be used not only for general understanding of heat transfer behavior but also, and even more importantly, for actual design of heat-exchange devices.

References

Campo, A. and Lacoa, U. 1987. The simplest approach to forced convection in horizontal pipes exposed to natural convection and radiation. *Int. Comm. Heat Mass Transfer*, **14**, 551–560

Gnielinski, V. 1989. Zur Wärmeübertragung bei Laminarer Rohrströmung und Konstanter Wandtemperatur. *Chemie Ingenieur Technik*, **61**, 160–161

Hardy, G. H., Littlewood, J. E., and Polya, G. 1967. *Inequalities*. Cambridge Press, Cambridge, UK

Hausen, H. Z. 1943. VDI Beih. *Verfahrenstech*, **4**, 91

Incropera, F. P. and DeWitt, D. P. 1990. *Introduction to Heat Transfer*. John Wiley, New York, NY

Kays, W. M. and Crawford, M. E. 1980. *Convective Heat and Mass Transfer*. McGraw-Hill, New York, NY

Lacoa, U. and Campo, A. 1990. Laminar forced convection in vertical pipes exposed to external natural convection and external radiation: uncoupled/lumped solution. *Wärme-und Stoffübertragung*, **25**, 1–8

Ösizik, M. N. and Sadeghipour, M. S. 1982. Analytical solution for the eigenvalues and coefficients of the Graetz problem with third kind boundary condition. *Int. J. Heat Mass Transfer*, **25**, 736–739

Santos, C. A., Cotta, R. M., and Özisik, M. N. 1988. Laminar forced convection inside externally finned tubes. *Proc. Brazilian Heat Transfer Conference (ENCIT)*, Aguas de Lindoia, Sao Paulo, Brazil, 87–90

Sparrow, E. M. and Charmchi, M. 1980. Laminar heat transfer in an externally finned circular tube. *J. Heat Transfer*, **102**, 605–611

Vick, B. and Wells, R. G. 1986. Laminar flow with an axially varying heat transfer coefficient. *Int. J. Heat Mass Transfer*, **29**, 1881–1889

Vick, B., Beale, J. H., and Frankel, J. 1987. Integral equation solution for internal flow subjected to a variable heat transfer coefficient. *J. Heat Transfer*, **109**, 856–860

APPENDIX: Validation of the geometric-spatial-mean Biot Number Bi_g

An argument linked with the ideas of information theory that leads to the choice of the geometric-spatial-mean Bi_g will be explained next. Consider the distance D between the function $g(X)$ and the generalized spatial mean of g, $M_r(g)$, defined by

$$D(g, M_r(g)) = \left| \int_{-\infty}^{\infty} \log\left(\frac{g(X)}{M_r(g)}\right) p(X)\, dX \right| \tag{A1}$$

This equation serves to provide a logarithmic distance between $g(X)$ and $M_r(g)$, where it is clearly seen that $D \geqslant 0$ for all possible values of the index r. Consequently, the aim of this approach is to choose a numerical value of the index r so as to minimize $D(g, M_r(g))$.

Alternatively, Equation A1 may be rewritten as follows:

$$\begin{aligned} D(g, M_r(g)) &= \left| \frac{1}{(X_1 + X_2)} \left[X_1 \log\left(\frac{\mathrm{Bi}_1}{M_r(g)}\right) + X_2 \log\left(\frac{\mathrm{Bi}_2}{M_r(g)}\right) \right] \right| \\ &= \left| \log\left[\frac{(\mathrm{Bi}_1^{X_1} + \mathrm{Bi}_2^{X_2})^{1/(X_1+X_2)}}{M_r(g)} \right] \right| \end{aligned} \tag{A2}$$

Therefore, selecting the value $r = 0$ in Equation A2 yields the relation

$$(D(g), M_r(g)) = 0 \tag{A3}$$

which in fact corresponds to the choice of the geometric-spatial-mean Bi_g given by Equation 11.

In addition, since $(D(g), M_r(g)) \geqslant 0$, it follows that Bi_g minimizes Equation A1. Hence, this argument tacitly demonstrates that the geometric-spatial-mean Bi_g (supplied by the logarithmic distance D of Equation A1) is indeed an optimal choice for the lower bound. Conceptually speaking, it provides the appropriate measure of the deviation from the function

$g(X)$. In essence, this logarithmic distance, rather than the variance, is strongly suggested by the exponential shape of the temperature distribution $T(x, r)$ in the fluid domain, i.e., the solution of the energy equation written in differential form (Kays and Crawford 1980).

Ultimately, upon combining Equations 12a and 14, it follows that D becomes

$$D(g, \mathrm{Bi}_a) = \left|\log\left(\frac{\mathrm{Bi}_g}{\mathrm{Bi}_a}\right)\right| = \log\left(\frac{\mathrm{Bi}_g}{\mathrm{Bi}_a}\right) \qquad \text{(A4)}$$

By virtue of this relation, a comparison of the performance of Bi_g with respect to Bi_a may be easily established. As it turns out, whenever D in Equation A4 is not negligible, this argument is a good indication that the choice of Bi_g, in conjunction with Bi_a, is superior and will improve the approximation significantly.